NeuroImage 54 (2011) 2672–2682

Contents lists available at ScienceDirect

NeuroImage

journal homepage: www.elsevier.com/locate/ynimg

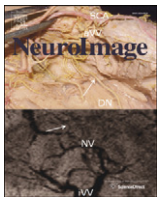

Thalamocortical changes in major depression probed by deconvolution and physiology-based modeling

Cliff C. Kerr [a,b,c,*], Andrew H. Kemp [d], Christopher J. Rennie [a,b,e], Peter A. Robinson [a,b]

[a] School of Physics, University of Sydney, New South Wales, Australia
[b] Brain Dynamics Centre, Westmead Millennium Institute, Sydney Medical School, Western, University of Sydney, Westmead Hospital, New South Wales, Australia
[c] Neurosimulation Laboratory, Downstate Medical Center, State University of New York, Brooklyn, NY 11203, USA
[d] School of Psychology, University of Sydney, New South Wales, Australia
[e] Department of Medical Physics, Westmead Hospital, Westmead, New South Wales, Australia

ARTICLE INFO

Article history:
Received 25 June 2010
Revised 22 October 2010
Accepted 1 November 2010
Available online 10 November 2010

Keywords:
Major depression
Melancholic subtype
Auditory event-related potential
Thalamocortical
Mean-field modeling
Deconvolution

ABSTRACT

Auditory event-related potentials (ERPs) have been extensively studied in patients with depression, but most studies have focused on purely phenomenological analysis methods, such as component scoring. In contrast, this study applies two recently developed physiology-based methods-fitting using a thalamocortical model of neuronal activity and waveform deconvolution — to data from a selective-attention task in four subject groups (49 patients with melancholic depression, 34 patients with non-melancholic depression, 111 participants with subclinical depressed mood, and 98 healthy controls), to yield insight into physiological differences in attentional processing between participants with major depression and controls. This approach found evidence that: participants with depressed mood, regardless of clinical status, shift from excitation in the thalamocortical system towards inhibition; that clinically depressed participants have decreased relative response amplitude between target and standard waveforms; and that patients with melancholic depression also have increased thalamocortical delays. These findings suggest possible physiological mechanisms underlying different depression subtypes, and may eventually prove useful in motivating new physiology-based diagnostic methods.

Introduction

Major depression is a highly heterogeneous illness (Parker et al., 2000; Mahli et al., 2005), associated with symptoms including anhedonia, psychomotor retardation, difficulties in concentrating, changes in appetite or weight, and suicidal ideation. Since attentional deficits are a common feature in most depressive illnesses (Hasler et al., 2004), auditory oddball event-related potentials (ERPs) are an obvious method of investigation. Using a relatively large sample of depressed participants, we previously reported increased standard and target P2 amplitudes, decreased P3 amplitudes, and increased P3 latencies (Kemp et al., 2009, 2010). This study aims to examine the physiological basis for these changes using physiology-based modeling (Kerr et al., 2008) and signal analysis techniques (Kerr et al., 2009).

Attempts to quantify changes in ERP waveforms using conventional methods, such as component scoring, have yielded contradictory results (e.g., el Massioui and Lesèvre, 1988; Sandman et al., 1992; Giese-Davis et al., 1993). The most consistent finding in patients with depression is reduced P3 amplitude (Kemp et al., 2009, 2010; Roth et al., 1981; Blackwood et al., 1987; Gangadhar et al., 1993; Bruder et al., 1995, 1998; Urretavizcaya et al., 2003); all other changes were reported by fewer than half of previous studies, potentially as a consequence of the heterogeneity of the disorder. Additionally, component scoring may not adequately quantify some of the changes that occur in patients with depression, since this method considers only a handful of data points from each ERP. Furthermore, given that source activations underlying ERP waveforms almost certainly overlap in time, changes in either amplitude or latency of one source may produce changes in *both* amplitude and latency of one or more components. For example, increases in target P2 amplitude (Kemp et al., 2009; Vandoolaeghe et al., 1998) and increases in target N2 latency (Kemp et al., 2010; Sandman et al., 1992; Urretavizcaya et al., 2003) could both result from a single amplitude or latency change in an underlying source.

Although many studies have reported changes in ERPs associated with depression, no clear physiological explanation of these changes has yet been advanced. This study applies two recently-developed techniques — deconvolution of target waveforms into overlapping standards, and fitting using a thalamocortical model of brain activity — to ERPs from four subject groups (melancholic depression, non-melancholic depression, subclinical depressed mood, and healthy

* Corresponding author. Complex Systems Group, School of Physics A29, University of Sydney, NSW 2006, Australia. Fax: +61 2 9351 7726.
E-mail address: ckerr@physics.usyd.edu.au (C.C. Kerr).

1053-8119/$ – see front matter © 2010 Elsevier Inc. All rights reserved.
doi:10.1016/j.neuroimage.2010.11.008

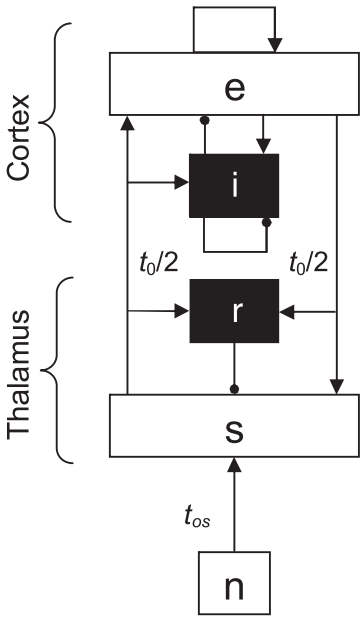

Fig. 1. The Robinson et al. thalamocortical model, consisting of five neuronal populations: cortical excitatory and inhibitory (*e* and *i*, respectively), thalamic reticular (*r*), thalamic sensory (*s*), and sensory afferents (*n*). The excitatory and inhibitory populations (white and black boxes, respectively) are linked by known anatomical connections (arrowheads for excitatory connections; circles for inhibitory). Time delays ($t_0/2$; t_{os}) are also shown.

controls), to obtain information on the pathophysiological changes underlying major depression.

Deconvolution (Kerr et al., 2009) re-expresses the target waveform in terms of the standard one, an approach motivated by the presence of similarities in the two waveforms (such as the N1 and P2 components). Empirically, targets are found to resemble a superposition of two amplitude-scaled standard waveforms, the second with a latency offset of ~100 ms. A physiological explanation is that target responses may be produced by the activation of two anatomically and dynamically similar cortical networks by thalamocortical (or corticocortical) impulses (Kerr et al., 2009). Deconvolution produces quantifications with much lower redundancy than component scores, and yields information about ERP waveforms not obtainable using conventional methods (Kerr et al., 2009).

The thalamocortical model developed by Robinson et al. (2001) is a physiology-based continuum model of spatiotemporal neuronal dynamics. In this model, neurons are grouped into five different subthalamic, thalamic, and cortical populations, and are interconnected via known anatomical connections, as shown in Fig. 1. Since electroencephalographic (EEG) activity is recorded at relatively large spatial scales, modeling individual neurons is unnecessary. Instead, neurons are described in terms of population-average properties (including synaptic strengths and axon lengths), which constitute the parameters of the model. This model has been successfully applied to a wide range of empirical data, including resting EEG spectra (Rowe et al., 2004), sleep dynamics (Phillips and Robinson, 2007), seizures (Roberts and Robinson, 2008), and Parkinson's disease (van Albada and Robinson, 2009; van Albada et al., 2009), as well as ERPs (Rennie et al., 2002; Kerr et al., 2008).

In this exploratory study, deconvolution and modeling are combined to provide complementary information on the thalamocortical system: for example, deconvolution peak latencies are related to time delays in the model, while deconvolution peak areas are related to connection strengths between neuronal populations. Thus, the application of both methods to the same data allows independent verification of changes in key parameters. For this reason, deconvolution and modeling benefit from conjoint use. However, the methods can also be used independently, as has been the case in previous work (Kerr et al., 2008, 2009, 2010).

Materials and methods

Participants

Age- and sex-matched patients with melancholic major depression ($n=49$) and non-melancholic major depression ($n=34$), participants with subclinical depressed mood ($n=111$), and healthy controls ($n=98$) were used in this study. Detailed group characteristics are given in Table 1; note that the same subject group was also recently investigated using ERP component scoring (Kemp et al., 2009, 2010). Participants were medication free for at least five half-lives, had no history of brain injury, loss of consciousness, stroke, neurological disorder, or other serious medical conditions, and provided written informed consent in accordance with National Health and Medical Research Council guidelines. The study was approved by the Sydney West Area Health Service and the University of Sydney Human Research Ethics Committees.

Participants with major depression were recruited by clinicians and community advertising. Diagnoses of melancholic and non-melancholic depression were made by trained personnel using the Mini-International Neuropsychiatric Interview (Sheehan et al., 1998), and severity of major depression was determined using the Structured Interview Guide for the Hamilton Depression Rating Scale (SIGH-D [Hamilton, 1960; Williams, 1988]). Non-patient participants were recruited by community advertising and were excluded if they self-reported a history or presence of psychiatric illness. These participants were screened for Axis I disorders using the Somatic and Psychological Health Report questionnaire (Hickie et al., 2001). All participants completed the Depression, Anxiety, and Stress Scale (DASS-21 [Lovibond and Lovibond, 1995]), a self-report measure of depression, anxiety, and stress. Non-clinical participants were categorized with and without depressed mood using the DASS-21 depression scale. Both DASS-21 and SIGH-D measures of depression severity showed large and statistically significant differences between groups ($p \leq 0.001$, Kruskal–Wallis tests). Although the diagnosis of melancholic versus

Table 1
Means (standard deviations) of demographic and psychiatric measures for each subject group. f = female; m = male; C = controls; S = participants with subclinical depressed mood; N = patients with non-melancholic major depression; M = patients with melancholic major depression; DASS = Depression, Anxiety, and Stress Scale; SIGH-D = Structured Interview Guide for the Hamilton Depression Rating Scale ANOVA = analysis of variance.

Measure	Controls	Subclinical	Non-melancholic	Melancholic	Statistics (ANOVA)
Sample size	98	111	34	49	–
Age (years)	35 (11)	36 (11)	35 (10)	38 (13)	$F(3)=1.1$, $p=0.37$
Sex	55 f, 43 m	57 f, 54 m	17 f, 17 m	33 f, 16 m	$F(3)=1.3$, $p=0.26$
DASS					
Depression	2.0 (2.2)	16.9 (7.5)	24.8 (9.9)	29.5 (10.4)	$F(3)=189$, $p<0.001$, C<S<N<M
Anxiety	1.2 (1.9)	6.7 (6.4)	8.8 (7.7)	16.1 (10.2)	$F(3)=53$, $p<0.001$, C<S,N<M
Stress	4.3 (4.1)	14.3 (8.7)	18.8 (8.6)	23.9 (9.1)	$F(3)=79$, $p<0.001$, C<S<N<M
SIGH-D	–	–	18.8 (3.9)	21.2 (6.4)	$F(1)=12$, $p=0.001$, N<M

non-melancholic depression is not based on depression severity, it is generally accepted that the melancholic subtype is associated with greater depression severity (Parker, 2000).

Recording procedure

EEG data were provided via the Brain Resource International Database (www.brainresource.com; Gordon et al., 2005). Recordings were obtained at 26 electrode sites according to an extended International 10–20 system, with a 500 Hz sampling rate (low-pass filtered above 100 Hz) and an A/D precision of 0.06 μV, following previously published methods for acquisition and artifact removal (Rowe et al., 2004; Gordon et al., 2005). Electrode impedance was generally maintained below 5 kΩ. A NuAmps (Neuroscan) amplifier and averaged mastoid reference were used.

Subjects were presented binaurally, via headphones, with standard and target tones (500 and 1000 Hz, respectively), at 75 dB sound pressure level and each lasting 50 ms, with a constant interstimulus interval of 1.0 s. Subjects were instructed to ignore standard tones, but to respond to target tones by pressing buttons with the index finger of each hand. There were 280 standard (82%) and 60 target (18%) tones presented in pseudorandom order. Task duration was 6 min. EEG data were corrected offline for eye movements following previously published techniques (Gratton et al., 1983; Miller et al., 1988). ERPs were extracted from EEG recordings by averaging from 0.0 to 0.6 s relative to stimulus onset. For each trial, baseline voltage was defined to be the average voltage for the 300 ms period prior to stimulus onset. Target and standard responses were averaged separately.

Deconvolution

Deconvolution analysis of single-subject ERPs was performed according to the method developed in Kerr et al. (2009), which is summarized here. Deconvolution expresses the difference between standard and target waveforms, and is thus similar in motivation to the calculation of difference waves such as mismatch negativity. Unlike difference waves, deconvolution can be used in cases where the target waveform appears to contain time-shifted or amplitude-scaled standard waveforms. To perform deconvolution, standard and target waveforms are first transformed into the frequency domain. The ratio of these transforms is computed, with a Wiener filter term (Wiener, 1949) used to reduce noise. The ratio is then transformed back into the time domain. Mathematically, the procedure is

$$D = \mathcal{F}^{-1}\left[\frac{\mathcal{F}[T]}{\mathcal{F}[S]}\left(\frac{(\mathcal{F}[S])^2}{\mathcal{F}[S]^2 + 1/SNR}\right)\right]$$

where D is the deconvolution waveform, S is the standard ERP, T is the target ERP, SNR is the signal-to-noise ratio (which is a function of frequency), $\mathcal{F}$ denotes a Fourier transform, and $\mathcal{F}^{-1}$ denotes an inverse Fourier transform. The $1/SNR$ term is chosen to minimize noise; since it primarily acts as a low-pass filter, its precise form has little effect. The function SNR used here is identical to that used in Kerr et al. (2009), producing low-pass filter characteristics with a −3 dB point at approximately 30 Hz. As shown in Fig. 2, the deconvolution waveform typically contains two peaks; in terms of conventional ERP components, the first peak roughly corresponds to N1 and P2 features of the target waveform, while the second peak corresponds to N2 and P3.

Deconvolution peaks can be quantified in terms of their area and latency. The latency of a deconvolution peak corresponds to the *relative response latency* between standards and targets. For example, a feature occurring with the same latency in both waveforms will produce a peak in the deconvolution waveform with zero latency, while a feature appearing in targets earlier than in standards will result in a deconvolution peak with negative latency. Peak area corresponds to *relative response amplitude*; a feature with identical amplitude in standards and targets produces a deconvolution peak of unit area. In general, target features are larger in amplitude than those of standards, so deconvolution peak areas are usually greater than unity. While deconvolution measures (peak area and latency) resemble amplitude ratios or latency differences obtainable via component

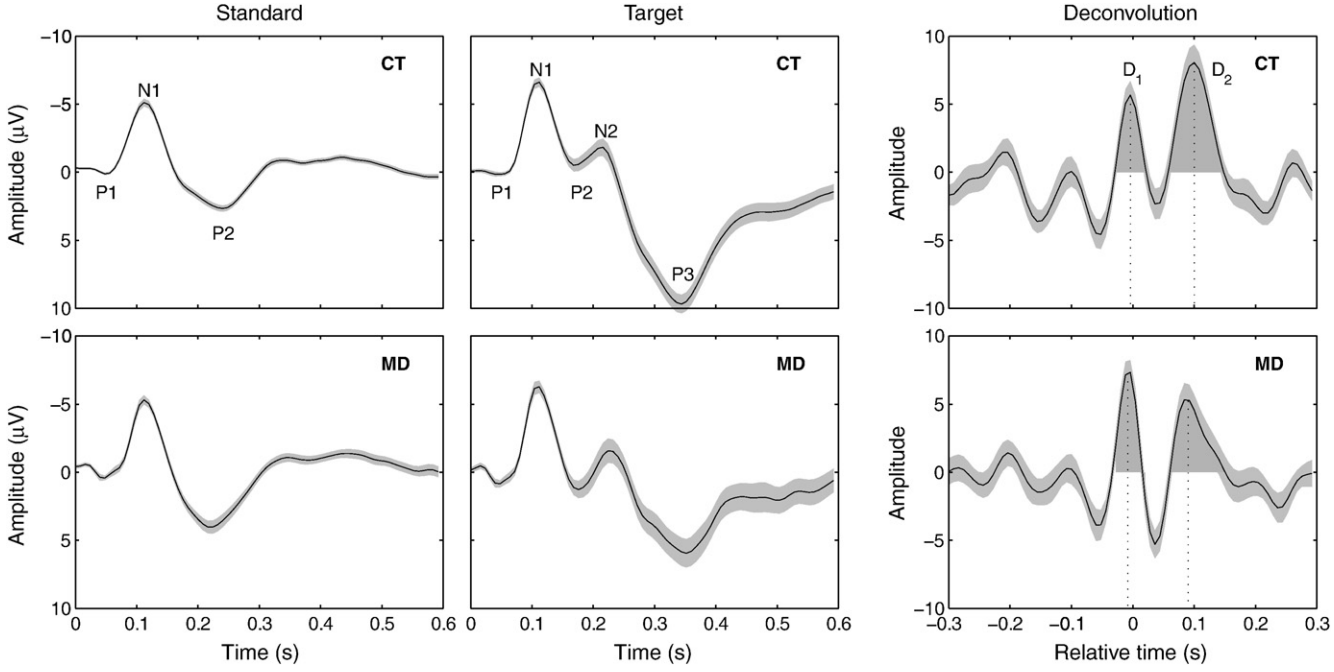

Fig. 2. Group average event-related potentials (ERPs) with standard errors (light gray), for controls ("CT", top row) and patients with melancholic depression ("MD", bottom row), recorded at Pz. Columns show standard ERPs (left), target ERPs (middle), and deconvolution waveforms (right). Key features of ERPs (P1, N1, P2, N2, and P3) and the deconvolution waveform (D_1 and D_2) are labeled for controls. Also shown are deconvolution peak quantifications, consisting of two latencies (dotted lines) and two areas (dark gray). Major differences between controls and patients with melancholic depression include decreases in D_2 peak area and P3 amplitude.

scoring, the major difference is that deconvolution uses the entire waveform, as opposed to isolated points, increasing its information content substantially (Kerr et al., 2009).

Model-based fitting

The model used here describes how average firing rates in different populations of neurons change over time. Since neuronal firing rates underlie scalp electrical activity, the model allows EEG and ERP data to be related to physiological and anatomical properties of the brain via the model's parameters. The model incorporates five different neuronal populations, as shown in Fig. 1: excitatory cortical pyramidal cells (denoted by subscript e), inhibitory cortical interneurons (i), excitatory thalamic relay nuclei neurons (s), inhibitory thalamic reticular nucleus neurons (r), and excitatory sensory afferents (n). Each population of neurons is described by its average properties, including firing rate, excitability, and axon length. Connections in the model, also shown in Fig. 1, include intracortical, intrathalamic, thalamocortical, and corticothalamic projections. The model also contains equations describing the dynamics of action potential propagation within dendrites and waves of activity spreading through the cortex.

To model evoked potentials, a brief subthalamic impulse (approximated by a spatiotemporally Gaussian function) is applied to the model, and the model's output–a prediction of the activity in cortical pyramidal cells–is fitted to the experimental ERP time series. This fit is performed by adjusting the model's parameters until the output of the model matches the major features of the experimental data to within uncertainty limits. Since full mathematical detail of the model has been presented elsewhere (Kerr et al., 2008), the remainder of this section qualitatively describes the model parameters and fitting method.

Parameters

There are 13 parameters in the model, listed in Table 2, but only five were varied to account for inter- and intra-subject variance in ERPs, as explained below. Model parameters can be divided into network parameters, stimulus parameters, and gains.

Network parameters describe key spatiotemporal properties of neuronal populations. The damping rate of cortical activity, γ, is defined as axonal propagation velocity divided by characteristic axonal range; its reciprocal characterizes the length of time waves of activity travel through the cortex before being damped. The thalamocortical signal propagation time, t_0, is the average time it takes an impulse to travel from the thalamus to cortex and back. The dendritic time constant, $1/\alpha$, is primarily determined by receptor kinetics (e.g., $GABA_A$ versus $GABA_B$), and has been described in previous work (Kerr et al., 2008) in terms of its reciprocal, α.

The stimulus in the model is a Gaussian impulse in both space and time, described by five parameters: spatial and temporal locations (relative to the point of measurement) r_{os} and t_{os}, respectively; spatial and temporal widths r_s and t_s, respectively; and amplitude N.

The strengths of connections between the neuronal populations shown in Fig. 1 are parameterized by gains. Gains are defined as the product of three properties of the neuronal populations: excitability (the extent to which changes in membrane potential cause changes in firing rate), the number of synapses involved, and average postsynaptic potential amplitude. Since these quantities can be measured experimentally, expected ranges can be obtained for each gain, although in practice these limits are quite large, as shown in Table 2. A gain G_{ab} describes the change in firing rate in neurons of population a resulting from a change in firing rate in neurons of population b. Positive gains represent excitation, and negative gains represent inhibition. For example, if a 30% increase in the firing rate of cortical neurons (e) is caused by a 10% increase in the firing rate of thalamic neurons (s), then $G_{es}=3$; if a 10% *decrease* in the firing rate of cortical neurons (e) is caused by a 10% increase in the firing rate of inhibitory neurons (i), then $G_{ei}=-1$. The gain across a chain of connections is the product of the individual gains, written as $G_{ab}G_{bc}=G_{abc}$. The 11 connections shown in Fig. 1 are grouped into five gains: the excitatory cortical gain G_{ee}, the inhibitory cortical gain G_{ei}, the excitatory thalamocortical gain G_{ese}, the inhibitory thalamocortical gain G_{esre}, and the inhibitory intrathalamic gain G_{srs}.

Fitting method

Fits were performed by varying the model parameters using the Levenberg–Marquardt method of maximizing goodness-of-fit (Press et al., 1992; Kerr et al., 2008). Initially, all 13 parameters were fitted; however, some parameters were poorly constrained by the present data. Parameters were subsequently fixed to given values if (i) they were strongly correlated with other parameters (i.e., Spearman's $\rho \approx 0.5$ for at least one pair); (ii) had little effect on the waveform (i.e., differences of value of up to a factor of two produced changes in the waveform of comparable magnitude to the uncertainty in the experimental data); or (iii) changed little between fits (i.e., fitted parameter values in >90% of fits were consistent with a single fixed value to within uncertainty). As a result, eight of the 13 parameters were fixed; the remaining five parameters were sufficient to explain both inter- and intra-subject variance. For each subject, fits were performed to both standard and target ERP waveforms at each of the 26 electrode sites.

The initial parameter values given in Table 2 had little effect on the final fitted values, and do not reflect "ideal" or maximum-likelihood values. Instead, they were chosen to reduce computation time by maximizing the fraction of fits that had acceptable goodness-of-fit. "Successful" fits were defined in terms of a χ^2 threshold; qualitatively, this threshold approximately corresponds to the model reproducing the N1, P2, and (for targets) N2 features to within experimental uncertainty. As discussed below, substantial increases in model complexity would be necessary to model the P3b component, and thus a requirement to reproduce P3 to within uncertainty was not imposed during fitting.

Table 2
Initial values and limits of model parameters used for fitting standard and target event-related potentials.

		Model[a]			Experiment[b]		
Parameter	Description	Initial	Min.	Max.	Min.	Max.	Unit
γ	Cortical damping rate	400	–	–	30	220[c]	s^{-1}
$1/\alpha$	Dendritic rate constant	70	20	100	5	200	ms
N^S or N^T	Amplitude normalization	6 or 10[d]	–	–	–	–	μV
t_0	Thalamocortical signal propagation time	70	50	90	9	100	ms
t_{os}	Temporal stimulus offset	15	–	–	–	–	ms
t_s	Temporal stimulus width	10	–	–	–	–	mm
r_{os}	Spatial stimulus offset	150	–	–	–	–	mm
r_s	Spatial stimulus width	45	–	–	–	–	mm
G_{ee}	Cortical excitatory gain	4.0	0.0	20	3	3000	–
G_{ei}	Cortical inhibitory gain	−10.0	–	–	−600	−0.4	–
G_{ese}	Thalamocortical excitatory gain	5.0	0.0	20	0	2000	–
G_{esre}	Thalamocortical inhibitory gain	−5.0	−20	0.0	-8×10^4	0	–
G_{srs}	Intrathalamic inhibitory gain	−4.0	–	–	−800	0	–

[a] Parameters whose limits are not given are fixed at the initial value.
[b] Data from Robinson et al. (2004).
[c] Value quoted for entire cortex; shorter axonal ranges (and thus higher cortical damping rates) would be expected in subnetworks, such as those responsible for generating event-related potentials.
[d] Parameter N fixed at values N^S and N^T for standard and target fits, respectively.

Statistics

A Shapiro–Wilk test showed that the null hypothesis of normal distributions of deconvolution quantifications and model parameters could be rejected in the majority of cases (63%). Hence, nonparametric statistical methods have been used throughout: values quoted are medians; the Kruskal–Wallis test has been used to determine if differences between subject groups for each parameter are statistically significant ($p<0.05$); and, if so, the Wilcoxon rank-sum test has been used to determine p values for differences between subject groups. The resultant p values are not further corrected for multiple comparisons for three reasons: (i) the Kruskal–Wallis test already controls for the effects of multiple comparisons between groups; (ii) key findings are validated using the split-half method (in which tests are performed on each half of the subject group, sampled randomly without replacement); and (iii) the present study is exploratory rather than prescriptive in nature. Statistical tests were implemented in MATLAB 7.7 (The MathWorks, Natick, Massachusetts).

Results

Deconvolution and modeling each yielded numerous statistically significant differences between groups. Key differences between healthy controls and clinical groups are summarized in Table 3, while the remainder of this section describes these results in detail.

Deconvolution

Deconvolution resulted in two peaks, as shown in Fig. 2, for 91% of waveforms; this fraction did not differ significantly between groups ($p>0.3$, binomial test). Deconvolution peak area and latency quantifications are shown in Fig. 3. In controls, deconvolution peak latencies were reasonably constant across the scalp, while deconvolution peak areas were not: the area of the first peak (D_1) was larger at frontotemporal sites (Fp1, Fp2, F7, F8, T3, and T4 vs. all other sites; Wilcoxon rank-sum test, $p=0.008$), while the area of the second peak (D_2) was larger at parietal and occipital sites than at frontal and central ones (all CP, P, and O sites vs. all Fp, F, FC, and C sites; Wilcoxon rank-sum test, $p<10^{-5}$). The latter result reflects the fact that the traditional P3 component, which contributes to D_2 area, has maximum amplitude over the posterior scalp (Johnson, 1989).

Kruskal-Wallis tests performed across all four groups found statistically significant inter-group differences in D_1 area ($p=0.0005$), D_2 area ($p<10^{-4}$), and D_2 latency ($p=0.02$), but not D_1 latency ($p=0.5$). For each of the three deconvolution quantifications that were found to differ significantly between groups, Wilcoxon rank-sum tests were performed between pairs of groups, as described in the remainder of this section.

Differences between participants with subclinical depressed mood and controls were typically small; the most notable differences were a scalp-average decrease in D_1 area of 6% (n.s.) and a 12% increase in D_2 area (n.s.). Major differences between non-melancholics and controls included a 19% decrease in D_1 area over the left hemisphere ($p=0.0003$) and a 15% increase in D_2 latency at prefrontal sites ($p=0.01$); the latter result should be interpreted with caution, however, given the relatively small number of sites that contribute to it. Compared to controls, non-melancholics also showed a decrease in D_2 area of 18% averaged across the scalp ($p=0.03$). Melancholics showed large decreases in D_2 area compared to controls (36% averaged across the scalp), and these decreases were highly significant ($p=0.0007$; for split-half analysis of both random subgroups, $p=0.01$ and 0.05). Melancholics also showed a 23% decrease in D_1 area ($p=0.002$).

Many of the findings described above remained statistically significant when compared to non-control groups. For example, D_2 latency at prefrontal sites differed between melancholic and non-melancholic groups ($p=0.003$), as well as between non-melancholics and participants with subclinical depressed mood ($p=0.02$). Decreases in D_1 and D_2 area did not differ significantly between melancholic and non-melancholic groups ($p>0.1$), but did differ between subclinical and clinical groups ($p=10^{-4}$ and 10^{-5} for D_1 and D_2, respectively; for each of the four split-half analyses, $p<0.006$).

Model fits

Successful fits (as determined by the goodness-of-fit threshold) were obtained for 97% of single-subject standard waveforms and 86% of single-subject target waveforms; examples of a wide range of successful fits are shown in Fig. 4. Parameter values for standard and target fits are shown in Figs. 5 and 6, respectively. Success rates of fits were independent of group ($p>0.2$, binomial test). Overall, parameter values for standard and target fits were similar in controls, with the exceptions of the thalamocortical gains, G_{ese} and G_{esre}: G_{ese} was more excitatory in targets, especially at central sites, while G_{esre} was more inhibitory, especially at parietal sites. The parameter showing the strongest scalp trend was G_{esre}, which varied from -3.5 at Fz to -14.8 at Oz in targets. Statistically significant group differences ($p<0.05$) were found for all parameters except for target G_{ese}, target G_{esre}, and standard G_{ee} (the last of which was nearly significant; $p=0.07$, Kruskal–Wallis test). The most significant group difference was found for target t_0 ($p=0.0009$, Kruskal–Wallis test).

Compared to controls, participants with subclinical depressed mood showed an 11% decrease in excitatory cortical gain G_{ee} in standards at central sites ($p=0.03$), a 110% increase in inhibitory thalamocortical gain G_{esre} in standards ($p=0.006$), and a 2.4% decrease in the dendritic time constant $1/\alpha$ in targets ($p=0.02$). Only two parameters differed between non-melancholics and controls: the dendritic time constant $1/\alpha$ was 3% lower in standard fits (n.s.) and 5% lower in target fits ($p=0.04$). The inhibitory thalamocortical gain G_{esre} in standards was an average of 60% larger in non-melancholics relative to controls over the right hemisphere ($p=0.05$).

The most notable finding for the melancholic group was increased thalamocortical signal propagation time t_0. Compared to controls, t_0 averaged 6% higher in melancholics for standard fits, and 22% higher for targets. Since t_0 is a very robust parameter, these differences

Table 3
Summary of depression-related changes in deconvolution quantifications and model parameters, relative to healthy controls. For the inhibitory gain G_{esre}, down arrows indicate more negative values (i.e., increased inhibition). If changes in model parameters differed between standard and target fits, the more statistically significant result is listed here.

Quantity	Description	Subclinical	Non-melancholic	Melancholic
D_1L	First deconvolution peak latency	–	–	–
D_1A	First deconvolution peak area	–	$\downarrow^{***}$	$\downarrow^{**}$
D_2L	Second deconvolution peak latency	–	$\uparrow^{**}$	–
D_2A	Second deconvolution peak area	–	$\downarrow^{*}$	$\downarrow^{***}$
$1/\alpha$	Dendritic rate constant	$\downarrow^{*}$	$\downarrow^{*}$	$\downarrow^{*}$
t_0	Thalamocortical signal propagation time	–	–	$\uparrow^{***}$
G_{ee}	Cortical excitatory gain	$\downarrow^{*}$	–	$\downarrow^{*}$
G_{ese}	Thalamocortical excitatory gain	–	–	$\downarrow^{**}$
G_{esre}	Thalamocortical inhibitory gain	$\downarrow^{**}$	$\downarrow^{*}$	$\downarrow^{*}$

– = n.s.; ↑ = increase; ↓ = decrease; $^{*}p<0.05$; $^{**}p<0.01$; $^{***}p<0.001$.

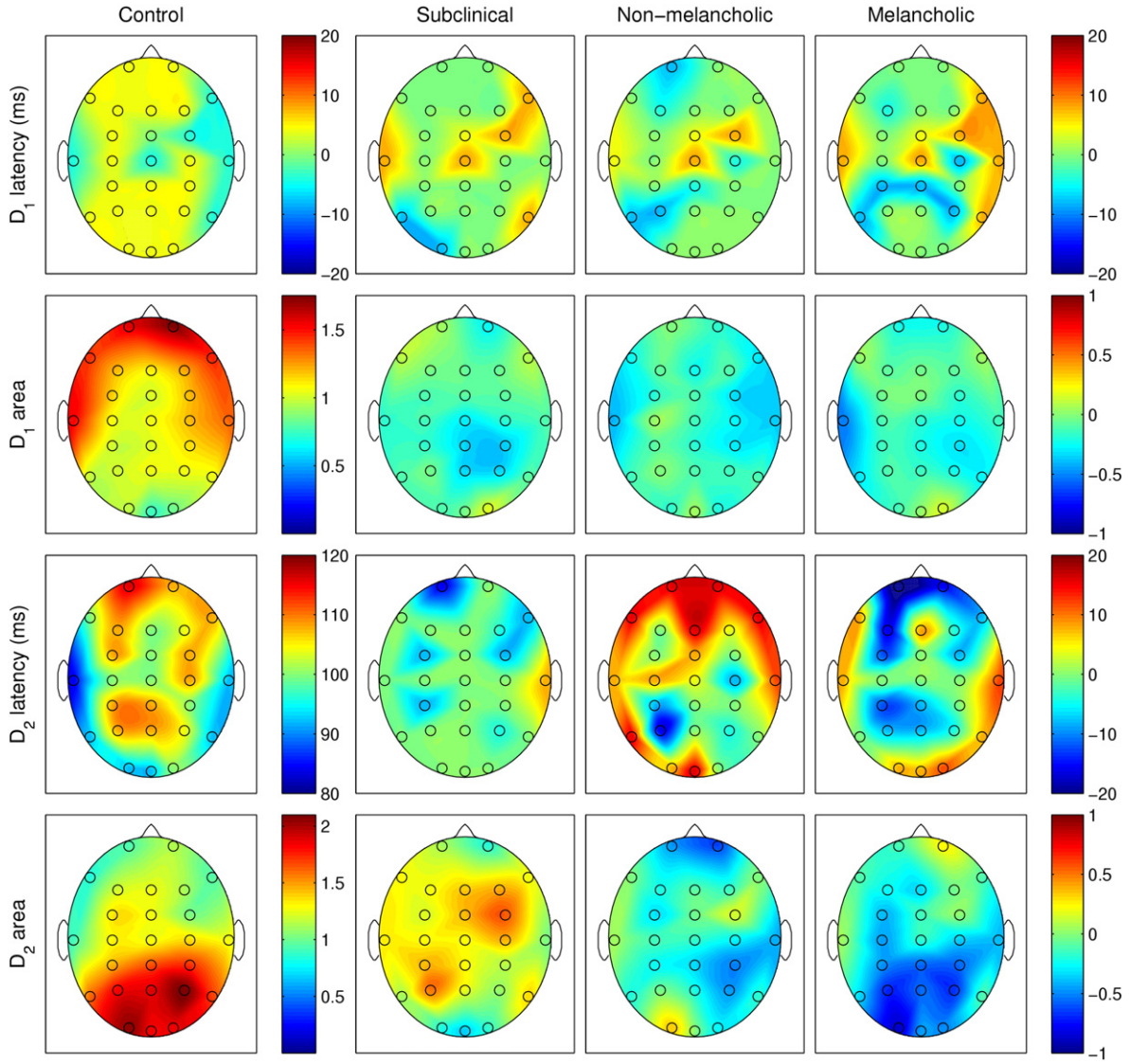

Fig. 3. Group average changes in the deconvolution peaks D_1 and D_2 (defined in Fig. 2). Each row shows a single quantity and its units (note that peak amplitude is dimensionless). The leftmost column shows results for healthy controls; the remaining columns show absolute differences between controls and subjects with subclinical, non-melancholic, and melancholic depression, respectively. Circles show electrode placement. Participants with subclinical depressed mood have increased D_2 area at right frontocentral sites; non-melancholics have increased D_2 latency at frontal sites, and moderately decreased D_1 and D_2 areas; melancholics show decreased D_2 area at parietal sites.

were highly significant ($p=0.002$ and $p=0.0001$ for standard and target fits, respectively; split-half analyses for target fits yield $p=0.004$ and 0.01). As predicted from the definition of t_0, there was a strong correlation between t_0 and reaction time (Spearman's $\rho=0.7$; $p<10^{-5}$). Strikingly, there was also a strong correlation between t_0 and SIGH-D scores (Spearman's $\rho=0.7$; $p<10^{-5}$). In comparison, reaction time and SIGH-D scores were only moderately correlated (Spearman's $\rho=0.2$; $p=0.02$).

All three gains also showed statistically significant differences between controls and melancholics: in standards, the excitatory thalamocortical gain G_{ese} was 45% less excitatory ($p=0.01$), while the inhibitory thalamocortical gain G_{esre} was 80% more inhibitory ($p=0.03$); in targets, the cortical gain G_{ee} was 16% less excitatory ($p=0.02$). Fractional decreases in the dendritic time constant $1/\alpha$ in standard and target fits were small (5% and 4%, respectively) but statistically significant ($p=0.02$ and 0.03, respectively). Differences in $1/\alpha$ were also significant when all participants with depressed mood, regardless of clinical status, were compared to healthy controls ($p=0.004$; for split-half analysis of both random subgroups, $p=0.03$ and 0.05).

Differences between subclinical participants and melancholics were comparable to differences between controls and melancholics, except for the thalamocortical gain G_{esre}, which showed no statistically significant differences between subclinicals and melancholics. Differences between subclinicals and non-melancholics were statistically significant ($p<0.05$) only at isolated electrodes; neither of the non-melancholic/control differences described above were significant between non-melancholics and subclinicals.

A subset of the statistically significant differences between melancholics and controls were statistically significant between melancholics and non-melancholics. The thalamocortical signal propagation time t_0 was larger in melancholics in both standard fits (5%, $p=0.03$) and target fits (17%, $p=0.008$), while the excitatory thalamocortical gain G_{ese} was 40% less excitatory ($p<0.04$).

Discussion

This is the first study to apply deconvolution-based signal analysis and physiology-based modeling to ERP waveforms recorded from patients with depression. Several striking differences between

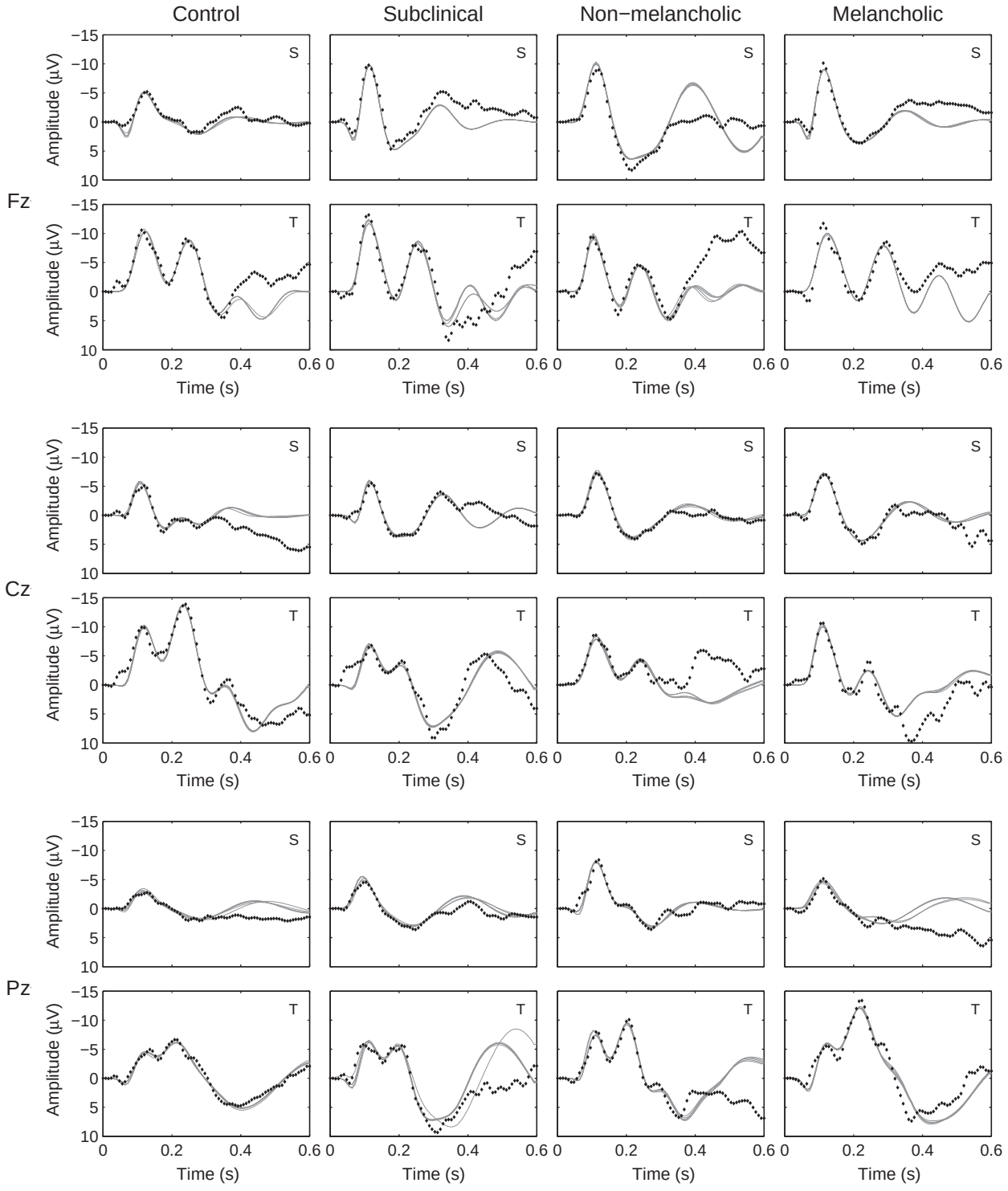

Fig. 4. Comparison of single-subject waveform data (dots) and the corresponding model fits (solid lines) to examples of standards (S) and targets (T), for three midline electrodes (rows), and for each subject group (columns). Large inter-subject, inter-group, and inter-electrode differences are visible, and are captured by model fits.

controls and other groups were observed. First, the relative response amplitude of targets versus standards at parietal sites decreased by 20–40% in patients with major depression, with more pronounced decreases found in melancholics. Second, the thalamocortical signal propagation time parameter increased by an average of 15 ms (20%) in melancholics, and was strongly correlated ($\rho = 0.7$) with depression severity in patients with major depression. Third, the dendritic time constant parameter decreased in all three clinical and subclinical groups, by an average of 4 ms (5%); in fits to standard ERPs, the correlation between the size of this decrease and the severity of depression approached statistical significance ($p < 0.1$, Spearman's correlation). Fourth, decreases in cortical excitation and/or increases in thalamocortical inhibition parameters of 20–30% were found in all groups with depressed mood, and additional decreases in thalamocortical excitation was found in melancholics. The following sections discuss the implications of these findings and the limitations of this study.

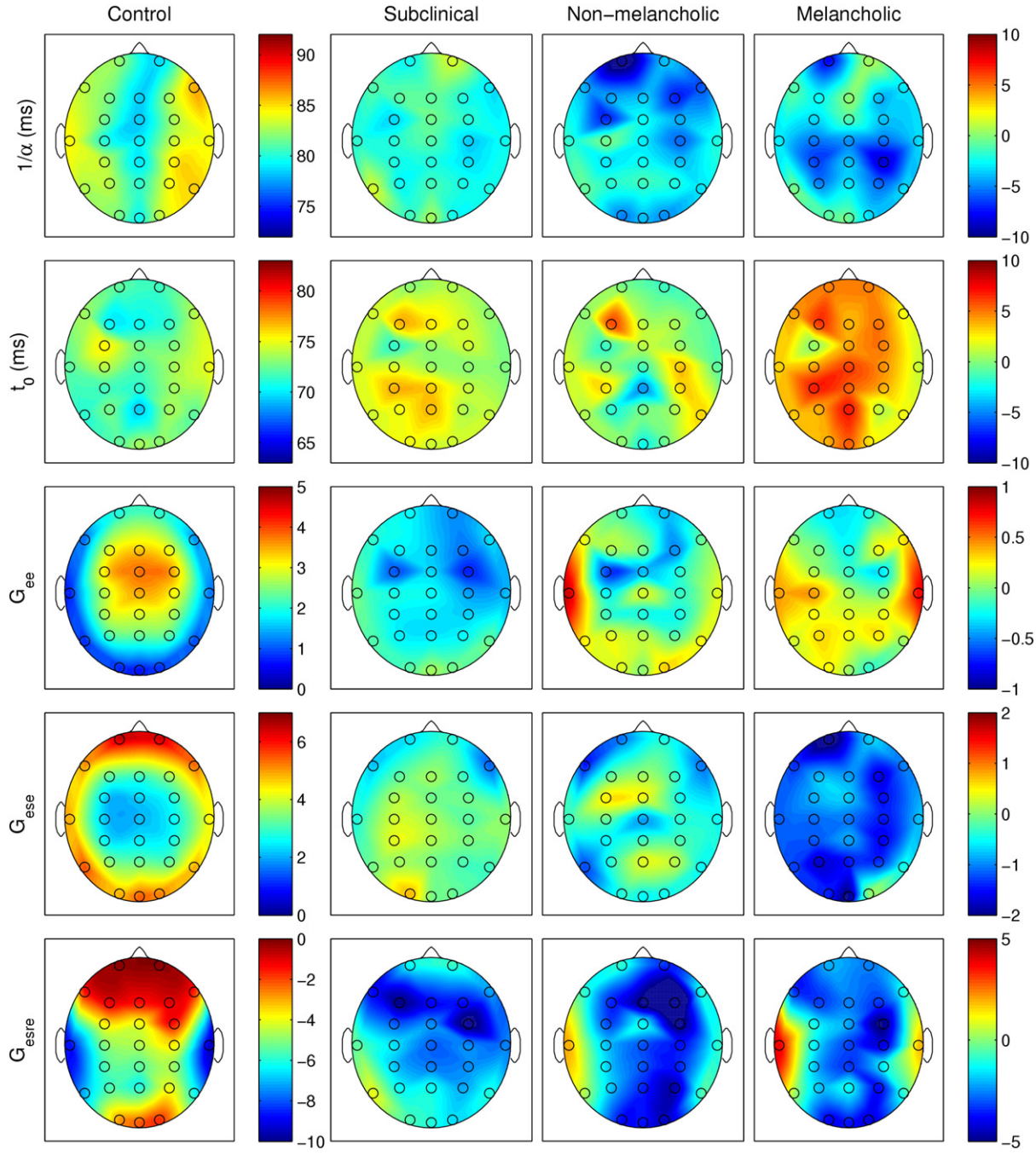

Fig. 5. Model parameters for standard fits. Each row shows a single model parameter and its units (note that gains are unitless). The leftmost column shows results for healthy controls; the remaining columns show absolute differences between controls and subjects with subclinical, non-melancholic, and melancholic depression, respectively. Major findings include decreased dendritic time constant $1/\alpha$ in both clinical groups, increased thalamocortical propagation time t_0 and decreased excitatory thalamocortical gain G_{ese} in melancholics, and increased magnitude of the inhibitory thalamocortical gain G_{esre} in all groups with depressed mood.

Deconvolution

The decreases in area of the second deconvolution peak (D_2) in patients with major depression can be largely attributed to P3 amplitude reduction (Blackwood et al., 1987; Bruder et al., 1995; Kerr et al., 2009); since P3 is maximal at posterior sites, this hypothesis also accounts for the predominantly posterior location of the group differences. However, the magnitudes of these decreases (20% in non-melancholics and 30% in melancholics) are larger than P3 amplitude changes typically found using oddball stimuli, and are more comparable to paradigms with complex stimuli and difficult task conditions (e.g., Bruder et al., 1995). Furthermore, using identical subjects, changes in D_2 area were found to be more significant than changes in P3 amplitude (e.g., $p = 0.007$ vs. $p = 0.04$, respectively, for control/melancholic differences at Pz) (Kemp et al., 2010).

The area of the first deconvolution peak decreased in non-melancholic participants; in contrast, component scores of the same subjects did not differ significantly from controls (Kemp et al., 2010), a result that demonstrates the sensitivity of deconvolution. Decreased area of the first deconvolution peak roughly corresponds to a reduced *difference* between standard and target N1 amplitude, which may be associated with the impaired orienting of attention found in patients with major depression (Paelecke-Habermann et al., 2005). Most studies have reported no significant effects of depression on

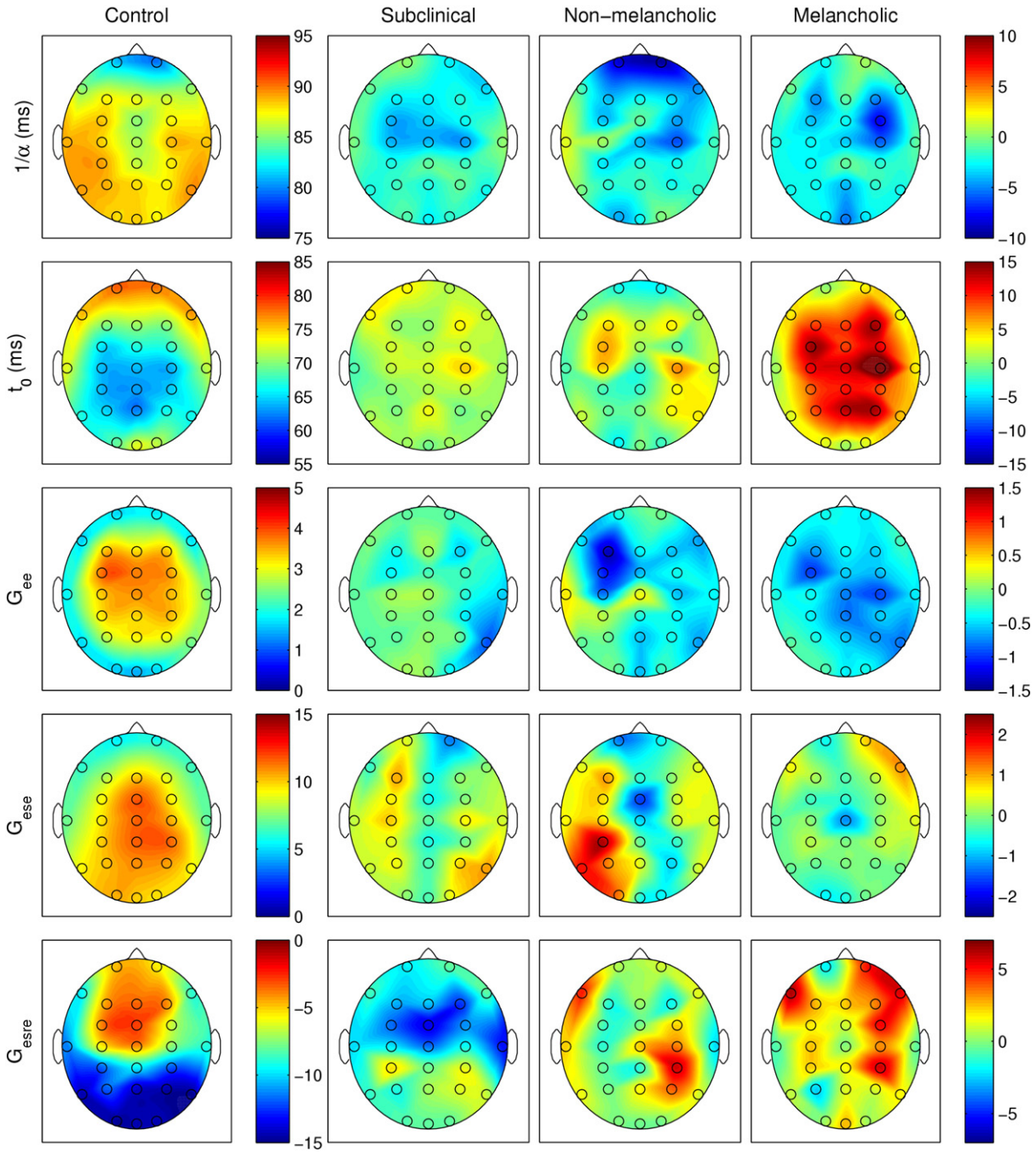

Fig. 6. Model parameters for target fits. Each row shows a single model parameter and its units (note that gains are unitless). The leftmost column shows results for healthy controls; the remaining columns show absolute differences between controls and subjects with subclinical, non-melancholic, and melancholic depression, respectively. Major findings include decreased dendritic time constant $1/\alpha$ and decreased excitatory cortical gain G_{ee} in all groups with depressed mood, and increased thalamocortical propagation time t_0 in melancholics.

N1 (e.g., Roth et al., 1981; Giese-Davis et al., 1993; el Massioui et al., 1996; Kemp et al., 2009), while others have found decreases in N1 amplitude (e.g., Yee et al., 1992; Burkhart and Thomas, 1993; Hansenne et al., 1996). However, to our knowledge, the finding of a decreased *difference* between standard and target component amplitudes has not been previously reported.

Modeling

Model fits to subjects with clinical and subclinical depression found a decreased dendritic time constant parameter ($1/\alpha$). Since the dendritic time constant is dominated by the neurotransmitter receptor time constant (Koch, 1999), a shift from NMDA receptors ($\tau \approx 100$ ms) to AMPA receptors ($\tau \approx 5$ ms) would be manifested in the model by decreased $1/\alpha$ (Forsythe and Westbrook, 1988). Indeed, evidence for such a shift has been found experimentally (Sanacora et al., 2008), since previous studies have reported decreases in NMDA receptor binding (Nudmamud-Thanoi and Reynolds, 2004), but no decrease in AMPA receptor binding (Beneyto and Meador-Woodruff, 2006). Additionally, evidence from animal models suggests that stress can decrease membrane time constants (Kole et al., 2004), although conflicting findings have also been reported (Holderbach et al., 2007).

The large increase in the thalamocortical signal propagation time parameter (t_0) in melancholics may partially explain the

psychomotor slowing associated with this subtype (Parker et al., 2000; Kemp et al., 2010). In the model, the target waveform is produced by multiple sequential thalamocortical loops, and we expect sequential loops would also be required in the production of the motor output. Since increases in t_0 of 10–15 ms across most of the scalp were observed, a motor response following three sequential thalamocortical loops would result in psychomotor retardation of 30–45 ms, consistent with the actual increase in reaction time of 49 ± 11 ms measured in these patients (Kemp et al., 2010). These results are also consistent with the finding of no change in deconvolution peak latencies, since increases in t_0 were found in both standard and target fits. The increase in t_0 may also underlie the component latency increases sometimes reported with depression (Urretavizcaya et al., 2003). The fact that changes in t_0 were large in patients with melancholic depression, but not in patients with non-melancholic depression, provides strong evidence that different neurophysiologic mechanisms contribute to these subtypes (i.e., dysfunction of intracerebral transmission only occurs in melancholic depression). A failure to distinguish melancholic and non-melancholic subtypes may thus explain many previously reported null findings regarding ERP latencies in depression.

Gains showed spatially widespread changes in clinical and subclinical groups, including decreased excitatory cortical gain G_{ee}, decreased excitatory thalamocortical gain G_{ese}, and increased inhibitory thalamocortical gain G_{esre}. On a group level, these gains can distinguish melancholics from non-melancholics (G_{ese} in standards), clinical patients from subclinical participants (G_{ee} in standards), and subjects with depressed mood from healthy controls (G_{esre} in standards). Several relationships between the changes in gain and changes in deconvolution peak area can be inferred: for example, in clinical and subclinical groups, right-hemisphere decreases in G_{ee} in target fits are consistent with right-hemisphere decreases in the area of the first deconvolution peak; in melancholics, increases in G_{ee} and decreases in G_{esre} in standard fits appear to contribute to decreases in the area of the second deconvolution peak.

Physiologically, it has recently been shown using an animal model that global reduction in serotonin availability shifts the balance of cortical activity from excitation towards inhibition: Moreau et al. (2010) artificially depleted serotonin levels in rat cortex, which resulted in a strong shift towards inhibition, due primarily to increased GABAergic currents. Although a significant body of evidence contradicts the simple monoamine deficit hypothesis of depression (Ressler and Nemeroff, 2000), dysfunction of the serotonin system remains a commonly reported correlate of depression, including in pathways involving the thalamus (Takano et al., 2007; Reimold et al., 2008). Such dysfunction offers a plausible explanation of the changes in cortical and thalamocortical excitability inferred by our model, especially with regard to the inhibitory thalamocortical gain G_{esre}. In addition, we predict that the observed changes in excitatory gains G_{ee} and G_{ese} may be associated with changes in NMDA- and AMPA-mediated transmission.

Limitations

The non-melancholic group was significantly smaller than other groups in this study, which may partially explain why only two differences between non-melancholics and controls were statistically significant across multiple electrodes. Furthermore, since the non-melancholic group may be comprised of patients with and without atypical depression, a feature not examined in this study, this group is likely to be the most heterogeneous (Mahli et al., 2005). Hence, additional psychiatric assessment, using specific tools to identify atypical depression (Stewart et al., 1993), is recommended for future work. Future work will also explore the relationships between model- and deconvolution-based parameters and key demographic and performance variables, including sex, years of education, and results from cognitive and behavioral tests.

It is undeniable that depression involves neurophysiological changes that cannot be captured by the comparatively simple model shown in Fig. 1. For example, P3 and other late-latency components typically involve complex interactions between brain regions (David et al., 2006), potentially including some that are not incorporated in the version of the model used here, such as the hippocampus (Halgren et al., 1998). In addition, the assumption of constant parameter values becomes less valid as time from stimulus onset increases, further limiting the ability of the model to account for late-latency features. These limitations explain the discrepancies between the experimental data and the model fits beyond 350 ms poststimulus, as seen in Fig. 4. However, we emphasize the model used here is the most complete of its kind yet available, and in most cases it successfully reproduces all major features of the observed ERP waveforms. While future refinements to the model may yield additional findings, the results presented here provide evidence of large-scale neurophysiological changes occurring in patients with major depression.

Conclusions

This work has presented several novel results regarding the pathophysiology of patients with depression inferred using noninvasive means, including evidence that: (i) patients with melancholic depression were found to have increased thalamocortical transmission delays, with the size of the increase strongly correlated with depression severity; (ii) all participants with depressed mood showed decreased amplitude differences between standard and target waveforms, indicating that attentional deficits are present within 100 ms poststimulus; and (iii) all participants with depressed mood showed decreased excitation and increased inhibition in the thalamocortical system. The high statistical significances of these results, and their direct physiological relevance, suggest their potential for clinical use in diagnosis or treatment selection, topics that will be explored in future work.

Acknowledgments

The authors acknowledge the data and support provided by BRAINnet (www.brainnet.net), which coordinates access to the Brain Resource International Database for independent scientific purposes, and thank the individuals who gave their time to participate in the study. CCK and PAR were supported by the Australian Research Council and Westmead Millennium Institute, and AHK by the National Health and Medical Research Council (Project Grant 464863 and Career Development Award 571101).

References

Beneyto, M., Meador-Woodruff, J.H., 2006. Lamina-specific abnormalities of AMPA receptor trafficking and signaling molecule transcripts in the prefrontal cortex in schizophrenia. Synapse 60, 585–598.

Blackwood, D.H., Whalley, L.J., Christie, J.E., Blackburn, I.M., St Clair, D.M., McInnes, A., 1987. Changes in auditory P3 event-related potential in schizophrenia and depression. Br. J. Psychiatry 150, 154–160.

Bruder, G.E., Tenke, C., Stewart, J.W., Towey, J.P., Leite, P., Quitkin, M., Voglmaier, F.M., 1995. Brain event-related potentials to complex tones in depressed patients: relations to perceptual asymmetry and clinical features. Psychophysiology 33, 373–381.

Bruder, G.E., Tenke, C., Towey, J.P., Leite, P., Fong, R., Stewart, J.W., et al., 1998. Brain ERPs of depressed patients to complex tones in an oddball task: relation of reduced P3 asymmetry to physical anhedonia. Psychophysiology 35, 54–63.

Burkhart, M.A., Thomas, D.G., 1993. Event-related potential measures of attention in moderately depressed subjects. Electroencephalogr. Clin. Neurophysiol. 88, 42–50.

David, O., Kiebel, S.J., Harrison, L.M., Mattout, J., Kilner, J.M., Friston, K.J., 2006. Dynamic causal modeling of evoked responses in EEG and MEG. Neuroimage 30, 1255–1272.

el Massioui, F., Lesèvre, N., 1988. Attention impairment and psychomotor retardation in depressed patients: an event-related potential study. Electroencephalogr. Clin. Neurophysiol. 70, 46–55.

el Massioui, F., Everett, J., Martin, M.T., Jouvent, R., Widlöcher, D., 1996. Attention deficits in depression: an electrophysiological marker. Neuroreport 7, 2483–2486.
Forsythe, I.D., Westbrook, G.L., 1988. Slow excitatory postsynaptic currents mediated by *N*-methyl-D-aspartate receptors on cultured mouse central neurones. J. Physiol. 396, 515–533.
Gangadhar, B.N., Ancy, J., Janakiramaiah, N., Umapathy, C., 1993. P300 amplitude in non-bipolar, melancholic depression. J. Affect. Disord. 28, 57–60.
Giese-Davis, J.E., Miller, G.A., Knight, R.A., 1993. Memory template comparison processes in anhedonia and dysthymia. Psychophysiology 30, 646–656.
Gordon, E., Cooper, N., Rennie, C.J., Hermens, D., Williams, L.M., 2005. Integrative neuroscience: the role of a standardized database. Clin. EEG Neurosci. 36, 64–75.
Gratton, G., Coles, M.G.H., Donchin, E., 1983. A new method for offline removal of ocular artifact. Electroencephalogr. Clin. Neurophysiol. 55, 468–484.
Halgren, E., Marinkovic, K., Chauvel, P., 1998. Generators of the late cognitive potentials in auditory and visual oddball tasks. Electroencephalogr. Clin. Neurophysiol. 106, 156–164.
Hamilton, M., 1960. A rating scale for depression. J. Neurol. Neurosurg. Psychiatry 23, 56–62.
Hansenne, M., Pitchot, W., Gonzalez-Moreno, A., Zaldua, I.U., Ansseau, M., 1996. Suicidal behavior in depressive disorder: an event-related potential study. Biol. Psychiatry 40, 116–122.
Hasler, G., Drevets, W.C., Manji, H.K., Charney, D.S., 2004. Discovering endophenotypes for major depression. Neuropsychopharmacology 29, 1765–1781.
Hickie, I.B., Davenport, T.A., Naismith, S.L., Scott, E.M., 2001. SPHERE: a national depression project. Med. J. Aust. 175 (Suppl), 1–55.
Holderbach, R., Clark, K., Moreau, J.-L., Bischofberger, J., Normann, C., 2007. Enhanced long-term synaptic depression in an animal model of depression. Biol. Psychiatry 62, 92–100.
Johnson, R., 1989. Developmental evidence for modality-dependent P300 generators: a normative study. Psychophysiology 26, 651–667.
Kemp, A.H., Hopkinson, P.J., Hermens, D.F., Rowe, D.L., Sumich, A.L., Clark, C.R., et al., 2009. Fronto-temporal alterations within the first 200 ms during an attentional task distinguish major depression, non-clinical participants with depressed mood and healthy controls: a potential biomarker? Hum. Brain. Mapp. 30, 602–614.
Kemp, A.H., Pe Benito, L., Clark, C.R., McFarlane, A., Mayur, P., Harris, A., et al., 2010. Impact of depression heterogeneity on attention: an auditory oddball event related potential study. J. Affect. Disord. 123, 202–207.
Kerr, C.C., Rennie, C.J., Robinson, P.A., 2008. Physiology-based modeling of cortical auditory evoked potentials. Biol. Cybern. 98, 171–184.
Kerr, C.C., Rennie, C.J., Robinson, P.A., 2009. Deconvolution analysis of target evoked potentials. J. Neurosci. Methods 179, 101–110.
Kerr, C.C., van Albada, S.J., Rennie, C.J., Robinson, P.A., 2010. Age trends in auditory oddball evoked potentials via component scoring and deconvolution. Clin. Neurophysiol. 121, 962–976.
Koch, C., 1999. Biophysics of Computation. Oxford University Press, New York.
Kole, M.H., Czeh, B., Fuchs, E., 2004. Homeostatic maintenance in excitability of tree shrew hippocampal CA3 pyramidal neurons after chronic stress. Hippocampus 14, 742–751.
Lovibond, S.H., Lovibond, P.F., 1995. Manual for the Depression Anxiety Stress Scales. Psychological Foundation, Sydney.
Mahli, G.S., Parker, G.B., Greenwood, J., 2005. Structural and functional models of depression: from sub-types to substrates. Acta. Psychiatr. Scand. 111, 94–105.
Miller, G.A., Gratton, G., Yee, C.M., 1988. Generalized implementation of an eye movement correction procedure. Psychophysiology 25, 241–243.
Moreau, A.W., Amar, M., Roux, N.L., Morel, N., Fossier, P., 2010. Serotoninergic fine-tuning of the excitation–inhibition balance in rat visual cortical networks. Cereb. Cortex 20, 456–467.
Nudmamud-Thanoi, S., Reynolds, G.P., 2004. The NR1 subunit of the glutamate/NMDA receptor in the superior temporal cortex in schizophrenia and affective disorders. Neurosci. Lett. 372, 173–177.
Paelecke-Habermann, Y., Pohl, J., Leplow, B., 2005. Attention and executive functions in remitted major depression patients. J. Affect. Disord. 89, 125–135.
Parker, G., 2000. Classifying depression: should paradigms lost be regained? Am. J. Psychiatry 157, 1195–1203.
Parker, G., Roy, K., Wilhelm, K., Mitchell, P., Hadzi-Pavlovic, D., 2000. The nature of bipolar depression: implications for the definition of melancholia. J. Affect. Disord. 59, 217–224.
Phillips, A.J., Robinson, P.A., 2007. A quantitative model of sleep–wake dynamics based on the physiology of the brainstem ascending arousal system. J. Biol. Rhythms 22, 167–179.
Press, W.H., Flannery, B.P., Teukolsky, S.A., Vetterling, W.T., 1992. Numerical Recipes in C. Cambridge University Press, Cambridge, U.K.
Reimold, M., Batra, A., Knobel, A., Smolka, M.N., Zimmer, A., Mann, K., et al., 2008. Anxiety is associated with reduced central serotonin transporter availability in unmedicated patients with unipolar major depression: a [^{11}C]DASB PET study. Mol. Psychiatry 13, 606–613.
Rennie, C.J., Robinson, P.A., Wright, J.J., 2002. Unified neurophysical model of EEG spectra and evoked potentials. Biol. Cybern. 86, 457–471.
Ressler, K.J., Nemeroff, C.B., 2000. Role of serotonergic and noradrenergic systems in the pathophysiology of depression and anxiety disorders. Depress. Anxiety 12 (Suppl 1), 2–19.
Roberts, J.A., Robinson, P.A., 2008. Modeling absence seizure dynamics: implications for basic mechanisms and measurement of thalamocortical and corticothalamic latencies. J. Theor. Biol. 253, 189–201.
Robinson, P.A., Rennie, C.J., Wright, J.J., Bahramali, H., Gordon, E., Rowe, D.L., 2001. Prediction of EEG spectra from neurophysiology. Phys. Rev. E 63, 021903.
Robinson, P.A., Rennie, C.J., Rowe, D.L., O'Connor, S.C., 2004. Estimation of multiscale neurophysiologic parameters by electroencephalographic means. Hum. Brain. Mapp. 23, 53–72.
Roth, W.T., Pfefferbaum, A., Kelly, A.F., Berger, P.A., Kopell, B.S., 1981. Auditory event-related potentials in schizophrenia and depression. Psychiatry Res. 4, 199–212.
Rowe, D.L., Robinson, P.A., Rennie, C.J., 2004. Estimation of neurophysiological parameters from the waking EEG using a biophysical model of brain dynamics. J. Theor. Biol 231, 413–433.
Sanacora, G., Zarate, C.A., Krystal, J., Manji, H.K., 2008. Targeting the glutamatergic system to develop novel, improved therapeutics for mood disorders. Nat. Rev. Drug Discov. 7, 426–437.
Sandman, C.A., Vigor-Zierk, C.S., Isenhart, R., Wu, J., Zetin, M., 1992. Cardiovascular phase relationships to the cortical event-related potential of schizophrenic, depressed, and normal subjects. Biol. Psychiatry 32, 778–789.
Sheehan, D.V., Lecrubier, Y., Sheehan, K.H., Amorim, P., Janavs, J., Weiler, E., et al., 1998. The Mini-International Neuropsychiatric Interview (M.I.N.I): the development and validation of a structured diagnostic psychiatric interview for DSM-IV and ICD-10. J. Clin. Psychiatry 59 (Suppl. 20), 22–57.
Stewart, J.W., McGrath, P.J., Rabkin, J.G., Quitkin, F.M., 1993. Atypical depression: a valid clinical entity? Psychopharmacology 16, 479–495.
Takano, A., Arakawa, R., Hayashi, M., Takahashi, H., Ito, H., Suhara, T., 2007. Relationship between neuroticism personality trait and serotonin transporter binding. Biol. Psychiatry 62, 588–592.
Urretavizcaya, M., Moreno, I., Benlloch, L., Cardoner, N., Serrallonga, J., Menchón, J.M., Vallejo, J., 2003. Auditory event-related potentials in 50 melancholic patients: increased N100, N200 and P300 latencies and diminished P300 amplitude. J. Affect. Disord. 74, 293–297.
van Albada, S.J., Robinson, P.A., 2009. Mean-field modeling of the basal ganglia-thalamocortical system. I. Firing rates in healthy and parkinsonian states. J. Theor. Biol. 257, 642–663.
van Albada, S.J., Gray, R.T., Drysdale, P.M., Robinson, P.A., 2009. Mean-field modeling of the basal ganglia-thalamocortical system. II. Dynamics of parkinsonian oscillations. J. Theor. Biol. 257, 664–688.
Vandoolaeghe, E., van Hunsel, F., Nuyten, D., Maes, M., 1998. Auditory event related potentials in major depression: prolonged P300 latency and increased P200 amplitude. J. Affect. Disord. 48, 105–113.
Wiener, N., 1949. Extrapolation, Interpolation and Smoothing of Stationary Time Series with Engineering Applications. M.I.T. Press, Cambridge, MA.
Williams, J.B., 1988. A structured interview guide for the Hamilton Depression Rating Scale. Arch. Gen. Psychiatry 45, 742–747.
Yee, C.M., Deldin, P.J., Miller, G.A., 1992. Early stimulus processing in dysthymia and anhedonia. J. Abnorm. Psychol. 101, 230–233.